

## Genetic control of male fertility in *Arabidopsis thaliana*: structural analyses of postmeiotic developmental mutants

P.E. Taylor<sup>1</sup>, J.A. Glover<sup>2\*</sup>, M. Lavithis<sup>1</sup>, S. Craig<sup>2</sup>, M.B. Singh<sup>1</sup>, R.B. Knox<sup>1,\*\*</sup>, E.S. Dennis<sup>2</sup>, A.M. Chaudhury<sup>2</sup>

<sup>1</sup>School of Botany, University of Melbourne, Parkville, Victoria 3052, Australia

<sup>2</sup>CSIRO Division of Plant Industry, GPO Box 1600, Canberra, ACT 2601, Australia

Received: 14 August 1997 / Accepted: 7 October 1997

**Abstract.** Seven new male-sterile mutants (*ms7–ms13*) of *Arabidopsis thaliana* (L.) Heynh. (ecotype columbia) are described that show a postmeiotic defect of microspore development. In *ms9* mutants, microspores recently released from the tetrad appear irregular in shape and are often without exines. The earliest evidence of abnormality in *ms12* mutants is degeneration of microspores that lack normal exine sculpturing, suggesting that the *MS12* product is important in the formation of pollen exine. Teratomes (abnormally enlarged microsporocytes) are also occasionally present and each has a poorly developed exine. In *ms7* mutant plants, the tapetal cytoplasm disintegrates at the late vacuolate microspore stage, apparently causing the degeneration of microspores and pollen grains. With *ms8* mutants, the exine of the microspores appears similar to that of the wild type. However, intine development appears impaired and pollen grains rupture prior to maturity. In *ms11* mutants, the first detectable abnormality appears at the mid to late vacuolate stage. The absence of fluorescence in the microspores and tapetal cells after staining with 4',6-diamidino-2-phenylindole (DAPI) and the occasional presence of teratomes indicate degradation of DNA. Viable pollen from *ms10* mutant plants is dehiscence from anthers but appears to have surface abnormalities affecting interaction with the stigma. Pollen only germinates in high-humidity conditions or during in-vitro germination experiments. Mutant plants also have bright-green stems, suggesting that *ms10* belongs to the *eceriferum* (*cer*) class of mutants. However, *ms10* and *cer6* are non-allelic. The *ms13* mutant has

a similar phenotype to *ms10*, suggesting is also an *eceriferum* mutation. Each of these seven mutants had a greater number of flowers than congenic male-fertile plants. The non-allelic nature of these mutants and their different developmental end-points indicate that seven different genes important for the later stages of pollen development have been identified.

**Key words:** Anther – *Arabidopsis* (mutants) – Development (microspore) – Male sterility – Mutant (*Arabidopsis*, male sterility) – Pollen (ultrastructure)

### Introduction

In higher plants, male fertility results from many individual developmental events that specify the ontogeny of the male organs such as the filaments and the anthers (stamens), as well as the development of the male gametophytes. Mutations that impair any step in these processes give rise to defective stamen or pollen development, and male sterility. Postmeiotic microspore development is specified by genes that are controlled by either the diploid sporophyte or the haploid gametophyte. Apart from a recent report of a male gametophytic mutant (Chen and McCormick 1996), gametophytic mutants have not been characterised as extensively as sporophytic mutants. However, the recent molecular cloning of gametophytically expressed genes and their inactivation in transgenic plants has led to gametophytic mutant phenocopies (Muschiatti et al. 1994). Characterization of sporophytic mutants that act after meiosis will enable us to determine the specific steps of postmeiotic microspore development that are controlled by these sporophytic genes.

A number of male-sterile (*ms*) mutants defective in various stages of microspore development have been isolated from angiosperms including *Arabidopsis* (Van der Veen and Wirtz 1968; Regan and Moffatt 1990; Chaudhury et al. 1992; Dawson et al. 1993; Goldberg

\*Present address: Research School of Biological Sciences, Australian National University, GPO Box 475, Canberra ACT 2601, Australia

\*\*Deceased

Abbreviations: DAPI = 4',6-diamidino-2-phenylindole; GUS =  $\beta$ -glucuronidase; *MS* = male-sterile (gene); SEM = scanning electron microscopy; TEM = transmission electron microscopy

Correspondence to: A. Chaudhury; Fax: 61 (6) 246 5000; E-mail: abdul@pican.pi.csiro.au

et al. 1993; Preuss et al. 1993; Chaudhury et al. 1994; Hülkamp et al. 1995; He et al. 1996; Peirson et al. 1996). Previously, we described the phenotype of four non-allelic *ms* mutants that impair either meiotic or premeiotic events. Here, we describe the phenotype of seven non-allelic *ms* mutants that are impaired in postmeiotic microspore development.

## Materials and methods

**Plant materials and mutant isolation.** Male-sterile mutants of *Arabidopsis thaliana* (L.) Heynh. were grown and isolated as previously described (Chaudhury et al. 1994). High-humidity conditions for the growth of *ms10* and *ms13* were maintained by placing plastic bags over the pots.

**Complementation analyses of male-sterile mutants.** Crosses were performed between the *MS/ms* heterozygote constructed from each of the male-sterile mutants with each of the *ms/ms* homozygous male-sterile plants. At least 50 F1 plants resulting from these crosses were scored for male sterility. Complementation analysis was also performed between the *ms10* mutant and *cer6-2* (in a Landsberg *erecta* background, obtained from the *Arabidopsis* Biological Resource Center). An *MS10/ms10* heterozygous plant was crossed with a *cer6-2/cer6-2* homozygous mutant plant and the F1 progeny scored for male sterility and the *cer* mutation. Complementation was also done with the early acting mutants that have been described earlier (Chaudhury et al. 1994).

**Microscopy.** Both light and transmission electron microscopy (TEM) of the mutants were performed as previously described (Chaudhury et al. 1994). For detection of nuclei, anthers were squashed in a mixture of 4',6-diamidino-2-phenylindole (1 mg·ml<sup>-1</sup>, DAPI), 0.1 M phosphate buffer, 1% Triton X-100 and 10% sucrose. Preparations were examined with a reflected-light fluorescence microscope (Olympus BH2-RFL) using UV exciter filters. For scanning electron microscopy (SEM) of *ms7*, *ms8* and *ms11* mutants, open flowers were fixed in 3% glutaraldehyde, 0.05 M Pipes buffer at pH 7 and post-fixed in 1% OsO<sub>4</sub>, dehydrated in ethanol and mounted on aluminium stubs with semi-dry conductive carbon paint. After critical-point drying with CO<sub>2</sub>, anthers were ruptured with a fine needle and sputter-coated with gold. Samples were viewed with a JSM 840 scanning electron microscope at 5–10 kV. The SEM analyses of *ms10* and *ms13* mutants were performed according to Craig and Beaton (1996). Open flowers were mounted on a flat support with conducting carbon paint and frozen under vacuum in a model E7400 cryotransfer unit (BioRad, Richmond, Calif., USA). After sputter-coating with gold, anthers were examined with a JEOL 6400 scanning electron microscope at 15 kV and –150 °C.

In-situ enzyme assays on 6- to 10- $\mu$ m-thick sections of whole buds embedded in Histo-resin were performed as previously described (De Block and Debrouwer 1992). Peroxidase is a marker of the sporophytic tapetum in the wild type and enables the stages of development and lyses of the tapetum to be followed. The peroxidase assay was used to localize peroxidases by indigo-blue precipitation. The reaction buffer consisted of 0.1 M citric acid, 0.2 M Na<sub>2</sub>HPO<sub>4</sub> at pH 5, 2 mM o-phenylenediamine and 0.003% H<sub>2</sub>O<sub>2</sub> (omitted for negative control). Sections were incubated at 24 °C for 5–15 min in the dark.  $\beta$ -Galactosidase is a marker of gametophytic gene expression in wild-type microspores and is also useful for targeting the stage of microspore degeneration in mutants. For  $\beta$ -Galactosidase, the indigogenic method was employed. These enzymes are involved in turnover of cell wall polysaccharides or catabolism of galactolipids (Singh and Knox 1984). The reaction buffer contained 50 mM citrate phosphate at pH 4.8, 2 mM potassium ferrocyanide, 2 mM potassium ferricy-

anide, 5% sucrose and 1.5 mM 5-bromo-4-chloro-3-indoxyl  $\beta$ -D-galactoside (X-gal, omitted for negative control) dissolved first in 1% dimethylformamide. The sections were incubated at 24 °C for 20 min in the dark.

**$\beta$ -Glucuronidase (*GUS*) assay.** Pollen from a *LAT52-GUS* homozygous plant (provided by Sheila McCormick, U.S. Department of Agriculture, Plant Gene Expression Centre, Albany, Calif.) was used to introduce this marker into each *ms* mutant line. F1 plants were initially grown under kanamycin selection, F2 seeds were collected from these plants, and F2 plants grown under kanamycin selection; kanamycin resistance is linked to the *LAT52-GUS* construct (Twell et al. 1990; Twell 1992). Male-sterile plants containing this construct were analysed for *GUS* expression. Flower buds with mature anthers prior to dehiscence from individual F2 plants (at least 10 per mutant) were stained in a mixture of 0.3% X-glucuronidase (5-bromo-4-chloro-3-indolyl- $\beta$ -D-glucuronic acid; Sigma, in 5% dimethylsulfoxide), 5 mM potassium ferricyanide, 0.3% Triton X-100 and 0.1 M phosphate buffer (pH 7.2) for at least 2 h at 37 °C (essentially as described by Jefferson et al. 1987). Preparations were viewed by brightfield microscopy. An early acting mutant, *ms4* (Chaudhury et al. 1994) was included as a control.

**Mapping.** To map the *ms11* mutation, *ms11* was crossed with a set of phenotypic-marker mapping lines for each of the five chromosomes obtained from the ABRC stock centre. The F1 progeny were self-pollinated and seeds harvested from individual plants. The F2 progeny were scored for male sterility and the various marker mutations. Initial data localized *ms11* to chromosome 4. The chromosome 4 marker line contained three homozygous mutations, *ap-2*, *bp-1* and *cer2-1*. For linkage analysis, recombination percentages were calculated using the product-ratio method of Stevens (1939) and converted to map units using Haldane's expression (Serra 1965).

**Pollen germination.** Germination medium (10% sucrose, 0.01% boric acid, 3 mM calcium nitrate and 0.7% agarose) was autoclaved and, just prior to use, microwaved and 50  $\mu$ l added to a well on a microscope slide. Flower buds with dehiscing anthers from wild-type, *ms10* and *ms13* plants were placed in contact with the medium. Upon removal, pollen remained attached to the slide, a coverslip was added and slides were enclosed in a sealed petri dish with moist filter paper (to ensure high relative humidity) and incubated at 22 °C for 18 h under constant illumination (150  $\mu$ mol · m<sup>-2</sup> · s<sup>-1</sup> Photosynthetically active radiation) in a growth cabinet. Slides were then examined by light microscopy. For in-vivo experiments with *ms10* and *ms13*, high humidity was maintained by covering pots with plastic film.

## Results

### Mutant isolation

Sterile mutant plants of *Arabidopsis* can be identified by the presence of seedless, short siliques. These plants can be classified as male-sterile if applying pollen from a wild-type fertile plant produces viable seed. The inflorescence has a flowering period of about three weeks and flowers open sequentially. Outcrossings were performed on various flowers of the inflorescence to verify that the sterility is a stable trait. Based on silique length, we identified 19 mutants that were male-sterile. Of these mutants, eleven were examined to determine the stages of development at which the microspores were arrested. Previously, we described four mutants which were defective in the male progenitor cells during, or prior

to, microsporocyte meiosis (Chaudhury et al. 1994). Here, we describe seven mutants in which the defect occurs after meiosis.

### Genetic analyses

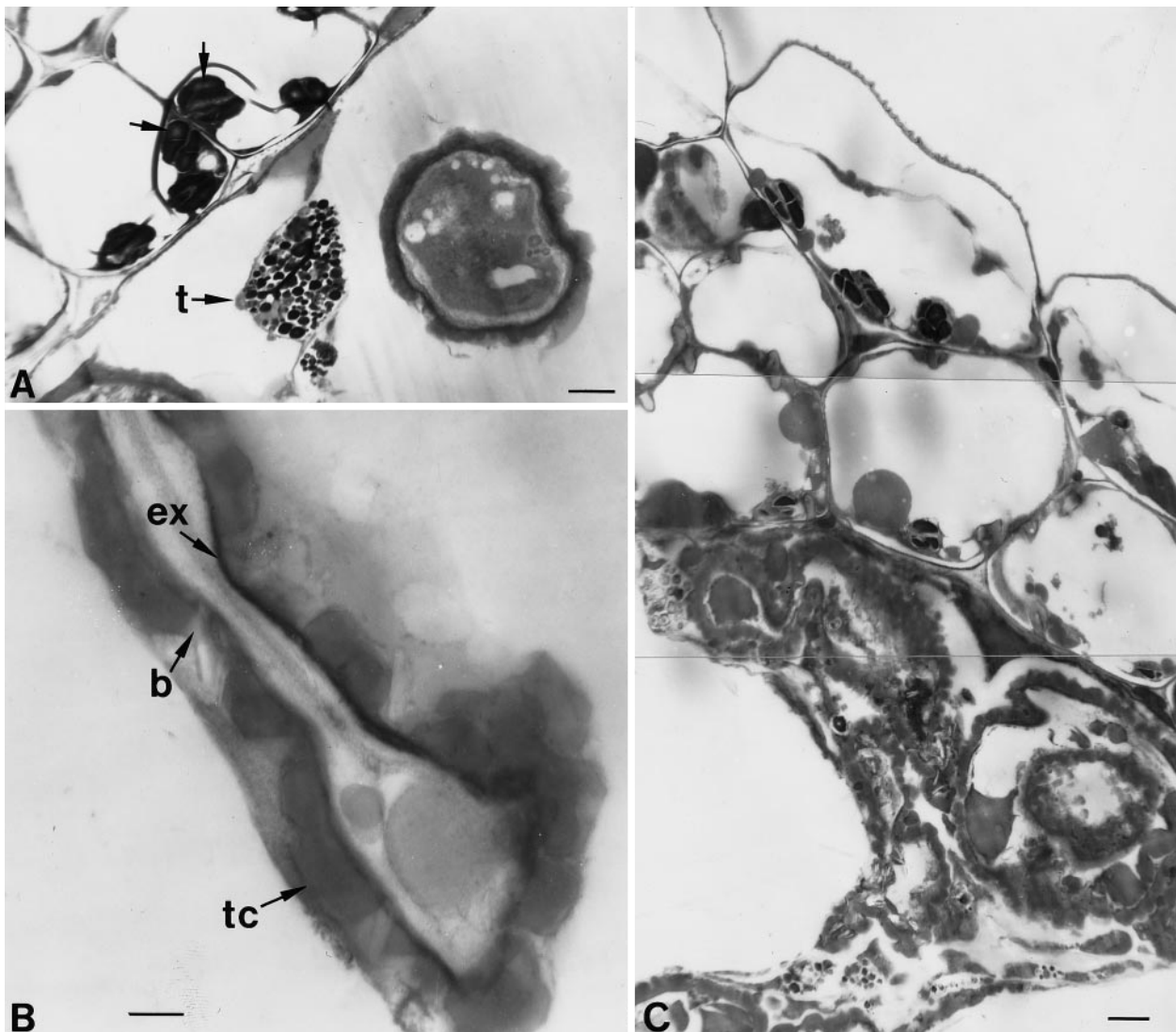
Each of the seven putative male-sterile mutants, designated *ms7*, *ms8*, *ms9*, *ms10*, *ms11*, *ms12* and *ms13* was rescued by pollination with self-fertile plants. The F1 plants from each of the *ms* mutants were grown and tested for male sterility based on their inability to form pollen and the length of the silique. Each

mutation proved to be recessive to the wild type, as demonstrated by the self fertility of the F1 plants. The F2 progeny of these F1 plants were scored for male sterility. Each of the mutations behaved as a single Mendelian locus.

### Genetic complementation

Pollen from *MS/ms* heterozygous plants of the seven male-sterile mutants was used to pollinate the same or a different *ms/ms* male-sterile plant to determine whether the mutants belong to the same or different complementation groups. The seven mutants represented seven different complementation groups since in all cases 100% of the F1 progeny from crosses between mutants were self-fertile. As expected, 50% of the progeny resulting from test-crosses between heterozygous plants and the same male-sterile mutant homozygotes were sterile. These mutants were also found to belong to complementation groups different from those defining the early acting mutants described previously (Chaudhury et al. 1994).

**Fig. 1A–C.** Transmission electron micrographs from sectioned anthers of *ms9*. **A** Wall formation of the microspores appears incomplete and the cytoplasm seems to be degenerating. The anther wall possesses many starch granules (*arrows*) and the tapetum (*t*) also degenerates. Bar = 2  $\mu$ m. **B** The wall of this microspore consists of an electron-opaque endexine (*ex*). However, the tectum (*tc*) lacks sculpturing and baculae cavities (*b*) are malformed. Bar = 500 nm. **C** At the next stage, the microspore contents have resorbed and the exine walls collapsed. Bar = 2  $\mu$ m



### Mapping of *MS11*

From the segregation data, *MS11* was located to chromosome 4. Segregants obtained when *ms11 CER2 AP2* was crossed in trans (repulsion) against *MS11 cer2 ap2* were as follows: *MS11 CER2* = 114; *ms11 CER2* = 41; *MS11 cer2* = 58, *ms11 cer2* = 1; *MS11 AP2* = 121; *ms11 AP2* = 39; *MS11 ap2* = 51; *ms11 ap2* = 3; *AP2 CER2* = 137; *ap2 CER2* = 18; *AP2 cer2* = 24; *ap2 cer2* = 35. Linkage analysis showed *MS11* to be 17.9 cM from *CER2* (SE  $\pm$  7.1 cM) and 39.8 cM from *AP2* (SE  $\pm$  6.7 cM). Since the segregants obtained showed the distance between *CER2* and *AP2* to be 27.9 cM (SE  $\pm$  3.3 cM), *MS11* is positioned to the north of *CER2*.

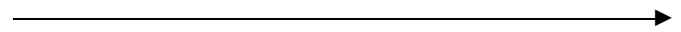
### Ultrastructural analyses

*ms9*. In this mutant, abnormalities first become detectable following the tetrad stage of development. The free microspores appear irregular in profile, often highly vacuolate, and surrounded by an electron-lucent wall and surface-adhering globular material of similar electron-opacity to the cytoplasm (Fig. 1A). The exine wall is not present at this stage and there is no cytochemically detectable  $\beta$ -galactosidase activity (data not shown). The tapetum is also degenerating and collapses without pollen coat formation (Fig. 1A). In the anther wall, the epidermis and endothecium are unusual in possessing a large number of starch granules (Fig. 1A). The wall of microspores contains endexine; however, proper sculpturing is impaired (Fig. 1B). In a different anther of the same mutant at a slightly later developmental stage, microspore contents appear to have leached out (Fig. 1C).

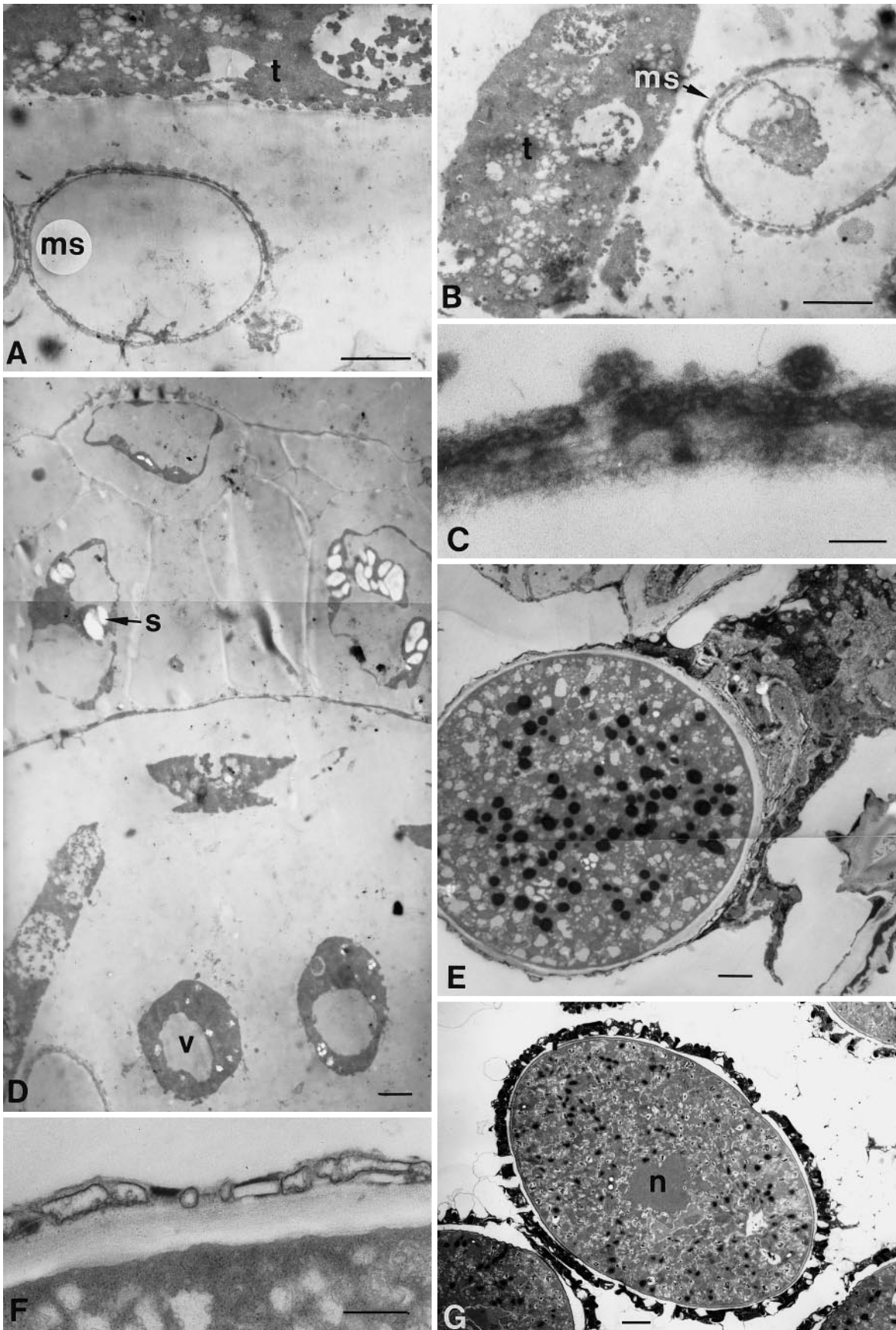
*ms12*. The earliest evidence of an abnormality in *ms12* is degenerating microspores that lack normal exine sculpturing either partially or completely (Fig. 2A–C). Microspores with partial exines have resorbed their cytoplasm yet remain turgid. The wall structure appears to be a bilayer with a continuous foot layer and globular connections, possibly representing early baculae. Other microspores without a detectable wall still retain cytoplasm including single large vacuoles and small starch granules (Fig. 2D). The tapetum degenerates at an early stage, just as plastids begin to differentiate into etioplasts. The anther wall contains many starch granules (Fig. 2D). Occasionally, teratomes are present in anther locules at later stages of development when the tapetum is degenerating. Teratomes contain cytoplasmic organelles bound by a spherical pollen wall consisting of an incompletely sculptured exine (Fig. 2E). The intine is uniform in thickness and apertures are not present (Fig. 2F). This abnormal cell is almost three to four times larger than the usual wild-type pollen grain (Fig. 2G). The teratome contains many small vacuoles and electron-opaque bodies probably consisting of lipids and phenolics. These are all larger than the similar

components found in wild-type pollen. Intact nuclei were not observed with TEM. The characteristics of *ms12* suggest an aberration occurring during the late tetrad period when the primexine is first formed around the microspores.

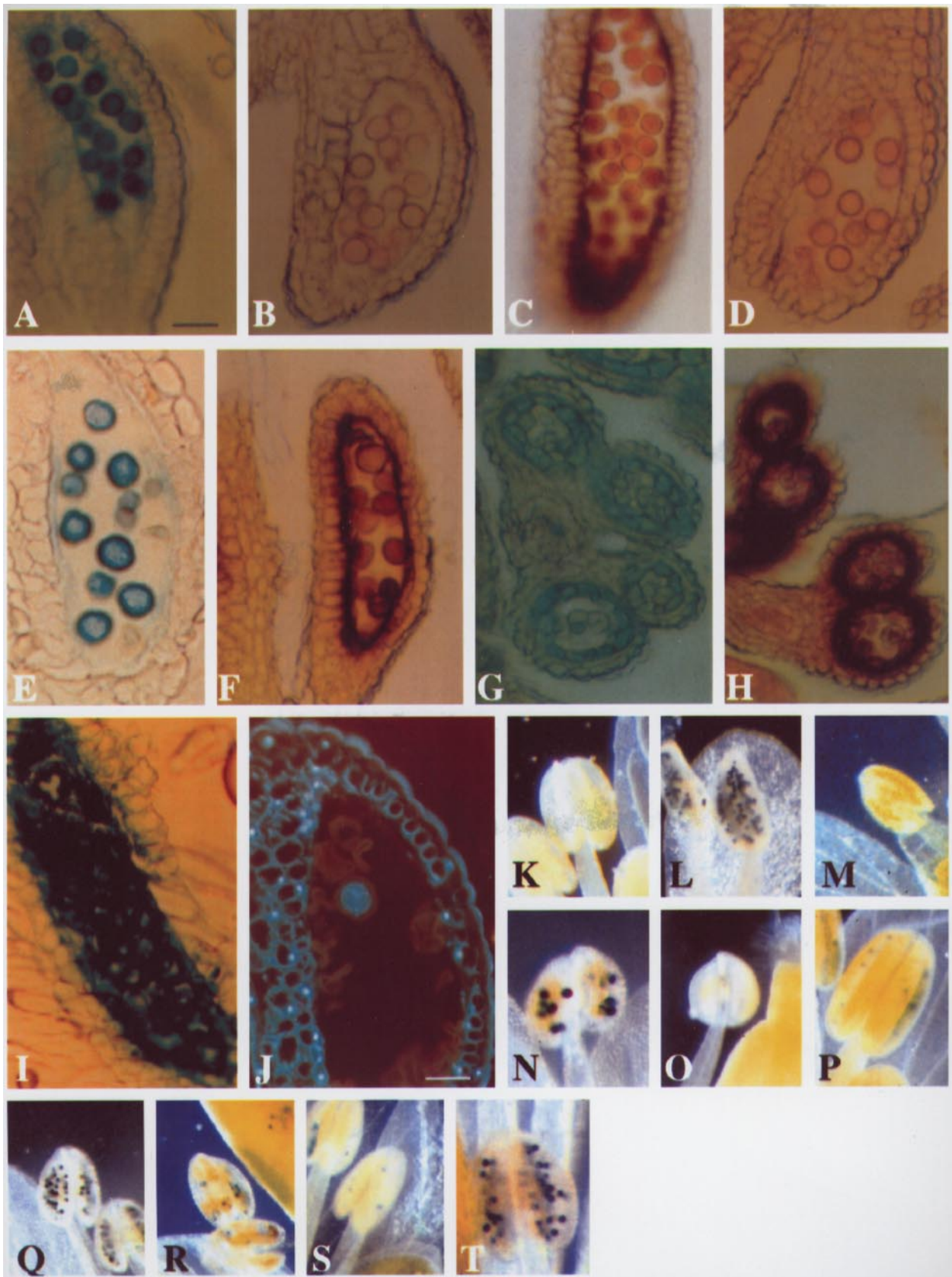
*ms7*. In the *ms7* mutant, microspores and tapetum appear similar to those of the wild type until the late vacuolate stage. In wild-type microspores and pollen grains,  $\beta$ -galactosidase occurs lightly in the tapetum and microspores and predominantly in the pollen grains (Fig. 3A); Fig. 3B shows the negative control. Peroxidase activity was predominantly localized within the intact tapetum with only light signal in the microspores (Fig. 3C; negative control, Fig. 3D). Cytochemical studies of  $\beta$ -galactosidase and peroxidase up to this stage show enzymatic activity and localization similar to the wild type (Fig. 3E,F).  $\beta$ -Galactosidase is active in the microspores and to a lesser extent in the tapetal cells, indicating that these cells are metabolically active. Within anthers of late vacuolate to early bicellular stages of the *ms7* mutant, the tapetal cells appear much thinner and have separated radially and begun to degenerate (Fig. 4A). At the early bicellular pollen stage, thin sections show a well-developed exine and there are several small vacuoles, amyloplasts with multigrain starch granules and electron-opaque bodies in the cytoplasm (Fig. 4B). Most pollen grains remain turgid and some have collapsed (Fig. 4C). In the vacuolate stage the wild-type anther contains four distinct layers of epidermis, endothecium, middle layer and tapetum (Fig. 4D). Wild-type microspores possess a large vacuole, a nucleus with nucleolus and a well-formed exine (Fig. 4E,F). Subsequently, the tapetal cytoplasm disintegrates with loss of membranes and the pollen cytoplasm appears highly vacuolate. Pollen grains then lyse, many appearing as empty shells with an intact exine and notably retaining their fully turgid shape. The cytoplasm of the anther wall cells (epidermis and endothecium)



**Fig. 2A–F.** Transmission electron micrographs of sectioned anthers of *ms12*. **A, B** Early in microspore development, some microspores (*ms*) have resorbed cytoplasm and incomplete wall formation and remain turgid. The tapetum (*t*) also appears to be degenerating and contains vacuoles, vesicles and plastids. Bars = 2  $\mu$ m. **C** Detail of the wall of a 'ghost' microspore showing incomplete development of tectum and baculae and absence of endexine. Bar = 200 nm. **D** The anther wall contains many starch granules (*s*), and occasionally wall-less microspores possessing a single vacuole (*v*) and starch granules are found in the loculus. Bar = 2  $\mu$ m. **E** At a later stage, a few enlarged microspores or teratomes remain intact in the loculus surrounded by many collapsed exine 'ghosts'. The teratomes possess vesicles, lipid bodies and mitochondria and are enveloped by an incomplete wall. Bar = 7  $\mu$ m. **F** Detail of the wall of a teratome showing incomplete tectum and baculae formation and absence of endexine below which the intine appears intact. Bar = 200 nm. **G** Transmission electron micrograph of sectioned anther of the wild type showing an ovoid pollen grain with an evaginated euchromatic vegetative nucleus (*n*). Pollen coat envelopes the exine and the pollen cytoplasm contains numerous electron-opaque lipid bodies and many small vesicles. Bar = 2  $\mu$ m







persists with chloroplasts possessing numerous large starch granules (Fig. 4A). Upon anther dehiscence, tapetal debris coats some of the sterile pollen grains. We conclude that in this mutant, the defect first becomes detectable during pollen development at the late vacuolate to early bicellular stage.

*ms8*. At the tetrad stage of *ms8* development, the tapetum and microspores appear similar to those of the wild type (data not shown). The tapetal cells have both low levels of  $\beta$ -galactosidase activity and intense peroxidase activity. Only weak activity for both enzymes occurs in the microspores (Fig. 3G,H). In the *ms8* mutant the locules contain empty flattened shells of pollen grains (Fig. 5A). The patterning of the pollen grain exine appears to be normal and continuous around the surface of the pollen grain, except at the apertures where it is absent or reduced as in the wild type (Fig. 5B). At the early vacuolate stage of microspore development, the uninucleate microspores have well-developed exines. Thin sections show that some microspores possess degenerated contents that have apparently ruptured (Fig. 5C). The tapetal layer has become thinner and cells radially separated, but the cytoplasm is electron-opaque, with abundant cytoplasmic contents

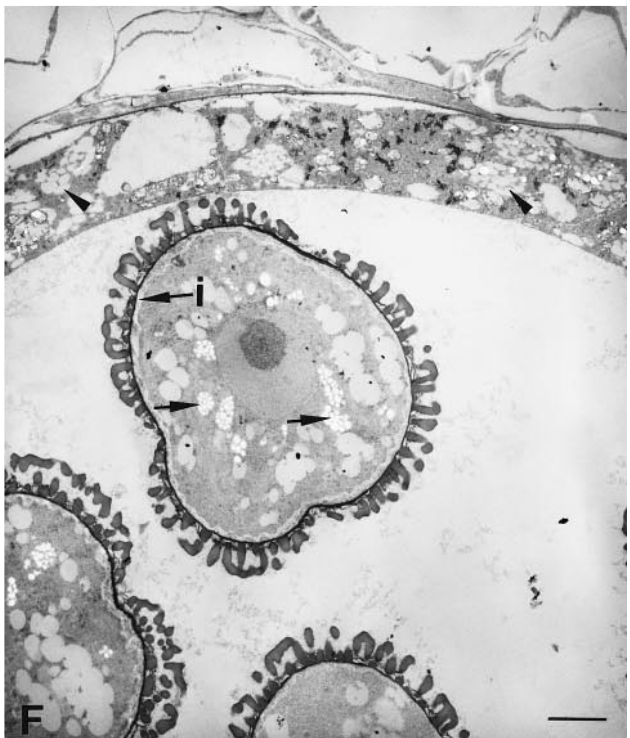
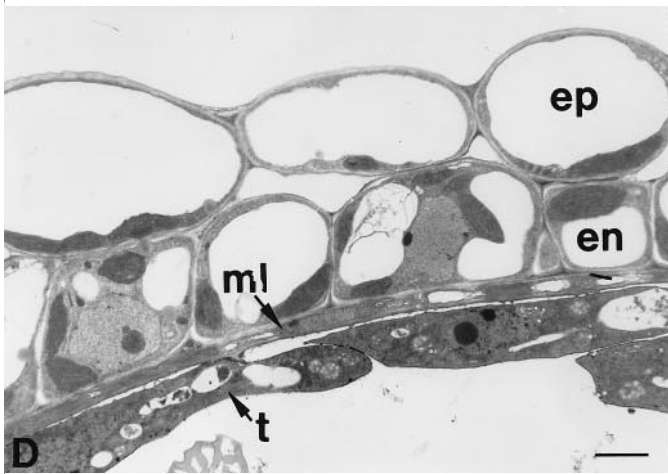
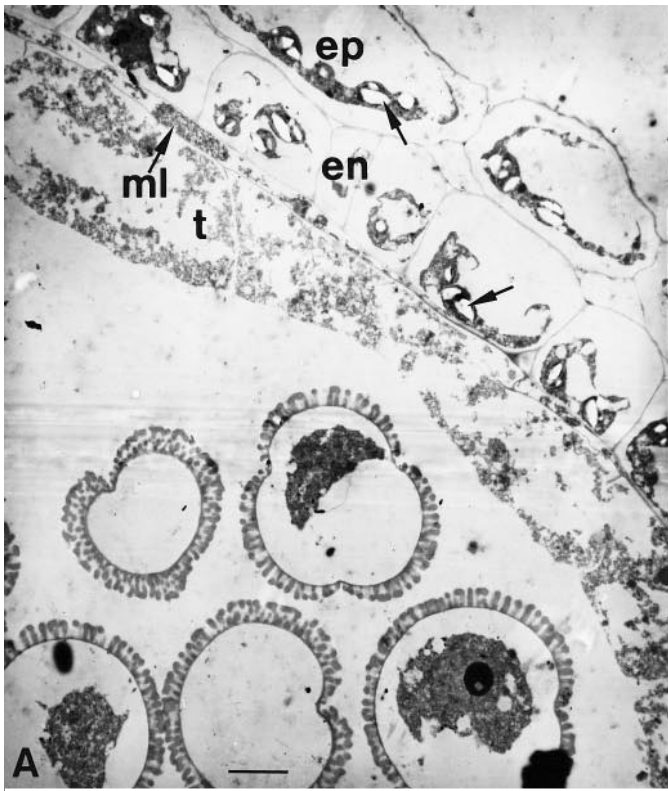
(Fig. 5D). In thin sections, the pollen grains comprised only exines and the pollen coat was not formed (Fig. 5E). Microspore ghost exines were also seen (Fig. 5E). However, the intine appears incomplete and development at the apertures is impaired.  $\beta$ -Galactosidase is detected mainly within the loculus, not in the microspores, perhaps due to their subsequent rupture (Fig. 3G). Anther wall cells appeared similar to those of the wild type (data not shown).

*ms11*. The first detectable abnormality appears in microspores at the mid to late vacuolate stage. Microspores appear highly vacuolate and exines are irregular and collapsed, although the exine tissue appears to be normal (Fig. 6A,B). The absence of fluorescence in the microspores and the tapetal cells after DAPI staining, apart from occasional teratomes or 'giant' pollen grains, indicates degradation of DNA (Fig. 3J). Cytochemically detectable  $\beta$ -galactosidase is diffused throughout the locule (Fig. 3I) and the tapetum is hypertrophied and degenerating. Auramine O fluorescence outlines a normal cuticle, wall thickenings in the endothecium, and stains the exine of both collapsed microspores and teratomes (results not shown). In thin sections, teratomes are spherical and appear to have a normal and granular cytoplasm with an almost fully developed exine (Fig. 6C). Collapsed microspores also exhibit a well-developed exine and occasionally have remnants of nuclei and cytoplasm (Fig. 6A,B). Anthers, containing teratomes and collapsed microspores, proceed to dehiscence (Fig. 6D).

*ms10*. Wild-type pollen germinating on stigmal papillae is shown in Fig. 7A,B. From SEM observations of *ms10* flowers, we confirm that pollen is dehisced from the anther but fails to germinate on the stigma (Fig. 7C,D). We detected abnormalities on the pollen surface in comparison to the wild type (data not shown). With the application of high humidity, pollen from the *ms10* mutant successfully germinates in vivo and forms homozygous mutant progeny. In vitro germination levels obtained for *ms10* pollen (18%) were within the range for wild-type pollen (10–30%). Another feature of *ms10* plants was the presence of bright-green stems, suggesting that it might be an eceriferum mutation. Similar to *ms10* mutants the *cer6* mutant has been reported to have bright-green siliques and to be male-sterile at low humidity (Preuss et al. 1993). Allelism tests were carried out between *ms10* and *cer6*. An *ms10*/*MS10* heterozygous plant was used as a pollen donor in a cross with a homozygous *cer6-2/cer6-2* plant that was also homozygous for the morphological mutation *erecta* that causes short stature. From 32 presumed F1 progeny scored, 3 were male-sterile but also had the *erecta* mutation as indicated by their shorter stature; since these plants showed maternal *erecta* phenotype they were not F1 and were not considered in the analyses of the complementation test. Each of the remaining 29 F1 plants was male-fertile indicating that *cer6* and *ms10* are not allelic. However, *ms10* could be allelic to a locus other than *cer6*.

←

**Fig. 3. A–I** Light micrographs from in-situ enzyme assays of sectioned anthers. Bar = 30  $\mu$ m. **A** Wild-type anther at the tricellular stage shows high levels of  $\beta$ -galactosidase within the pollen cytoplasm. **B**  $\beta$ -Galactosidase negative control. **C** Wild type, at the late vacuolate stage; peroxidase activity was mostly detected in the tapetum, with some staining in the pollen cytoplasm. **D** Peroxidase negative control. **E** The *ms7* mutant at the late vacuolate stage shows  $\beta$ -galactosidase activity in the microspore cytoplasm and, to a lesser extent, in the tapetum. **F** In sections from the same anther, peroxidase activity appears similar to that in the wild type. **G** At the late tetrad stage, the *ms8* mutant shows weak  $\beta$ -galactosidase activity both in the tapetum and microspores as is found in the wild type (data not shown). **H** In sections from the same flower, peroxidase staining is intense in the tapetum and activity is also detected in the microspores as is found in the wild type. **I** At the vacuolate microspore stage, the *ms11* mutant shows dispersal of  $\beta$ -galactosidase activity within both the loculus and the microspores. **J** Anther from an *ms11* mutant (DAPI staining). Fluorescence was not detected in the collapsed microspores or tapetal remnants. A teratome shows diffuse fluorescence of possibly degraded DNA. Anther wall cells, however, show sharply fluorescing nuclei. Bar = 45  $\mu$ m. **K–T** Expression of *LAT52-GUS* in whole anthers from wild-type and transformed wild-type plants and *ms* mutants. Anthers were taken from floral stage 10 to floral stage 13 flower buds (Bowman et al. 1991). **K** An untransformed fertile plant stained for GUS activity (negative control). No staining is visible in the anther. **L** A wild-type plant transformed with *LAT52-GUS* showing high levels of GUS activity in the pollen grains (positive control). **M** Anther from a premeiotic mutant, *ms4*, carrying a *LAT52-GUS* construct, showing no GUS staining. **N** Anther from *LAT52-GUS ms7* mutant showing GUS activity in only a few pollen grains of the anther. **O** Anther from *LAT52-GUS ms8* mutant showing no GUS staining. **P** In the *LAT52-GUS ms9* mutant, only a few pollen grains showed GUS expression. **Q** Anthers from *LAT52-GUS ms10* mutant plants show pollen staining similar to wild-type *LAT52-GUS* anthers. **R** Occasional GUS staining in the *LAT52-GUS ms11* anthers probably corresponds to the teratomes. **S** Anther from the *LAT52-GUS ms12* mutant showing a few GUS-stained teratomes. **T** Anthers from transformed *ms13* mutant plants showing high levels of GUS activity similar to the positive control (L)





*ms13*. Like *ms10*, pollen from *ms13* mutant plants dehisces from the anthers, but fails to germinate on the stigmatic papillae (Fig. 7E,F). Also like *ms10*, *ms13* pollen only germinates in vivo under high humidity. In vitro germination experiments show germination levels similar to that of *ms10* and wild-type pollen (11.2%). Staining with DAPI showed mutant pollen was tricolour (data not shown). The *ms13* mutants have a waxy phenotype (plants have bright-green stems), suggesting that this may also be a *cer* mutation. Allelism between *ms13* and *cer6* was not tested.

#### Expression of *LAT52-GUS* in the *ms* mutants

In order to help confirm the stage of action of the male-sterile mutants, the promoter activity of *LAT52* (a pollen-specific gene from tomato, Twell et al. 1990) was analyzed in these mutants. *LAT52* is expressed specifically in the vegetative cell of pollen in tobacco, tomato and *Arabidopsis* (Twell 1992; David Twell, Department of Biology, University of Leicester, UK, Personal communication). *ms4* is a pre-meiotic male-sterile mutant isolated and reported previously (Chaudhury et al. 1994). After crossing *ms4* mutant plants with transgenic plants containing the *LAT52* promoter fused to *GUS*, no *GUS* expression occurred (in contrast to the positive control, Fig. 3L), confirming that microspore development was disrupted prior to pollen mitosis I (Fig. 3M). Figure 3K is the negative control. In *ms7* mutants, only a few pollen grains in the anther stained for *GUS* (Fig. 3N). Anthers from crosses made with *ms8* were

also *GUS*-negative (Fig. 3O). This is consistent with our structural studies of *ms8* mutants which show that degeneration of microspores begins at the early vacuolate stage. The *ms9/LAT52-GUS* plants showed sporadic *GUS* staining, reflecting the heterogeneity of microspore developmental arrest (Fig. 3P). Pollen from the *ms10* mutant shows staining similar to that of the wild type (Fig. 3Q). From crosses with *ms11*, anthers appeared to possess several *GUS*-positive pollen grains. These are most likely the teratomes (Fig. 3R). The first structural abnormality in *ms11* appears in microspores at the vacuolate stage. These results suggest that most microspores did not undergo mitosis. Anthers from *ms12/LAT52-GUS* plants showed very few pollen grains stained for *GUS* (Fig. 3S). These also probably correspond to the teratomes. The *GUS* staining of *ms10/LAT52-GUS* and *ms13/LAT52-GUS* plants was comparable to that of positive control plants, supporting our other data that *ms10* and *ms13* are very late-acting mutants (Fig. 3Q,T).

#### Discussion

We have described seven sporophytic non-allelic mutations that impair microspore development after microsporocyte meiosis. Two mutants, *ms9* and *ms12*, appear to undergo developmental arrest either late in the tetrad or soon after microspore release. The other five mutations, *ms7*, *ms8*, *ms10*, *ms11* and *ms13*, affect later stages of microspore and pollen grain development (Fig. 8).

*Primexine mutations.* While some *ms12* microspores contained cytoplasm, others possessed only a partially complete exine and later, a few developed into 'giant' microspores or teratomes. These teratomes may have survived by out-competing for the limited resources from the tapetum. It is possible that the teratomes are microsporocytes that failed to undergo meiosis; their large size could be a result of their ploidy level (2n), causing them to out-compete microspores of lower ploidy (Heslop-Harrison 1971). In this case, the lack of a fully developed exine was not vital for survival in the anther, as the exine does not appear to progress beyond callose release and lacks either identifiable baculae or a reticulate pattern. Teratomes are only rarely found in wild-type plants. The teratomes of *ms12* have an intine surrounded by an amorphous layer probably having the advantage of permeability as the main asset for survival.

The heterogenous phenotype of *ms9* mutants also showed a developmental block at late tetrad stage. There is no patterned exine surrounding the vacuolate microspores and, instead, an accumulation of spherules of sporopollenin occurs. This suggests that developmental arrest may have occurred prior to the late patterned period which occurs within wild-type tetrads, when a form of sporopollenin is laid down over the primexine, after which all the intricacies of mature final wall patterning are completed (Heslop-Harrison 1968;

**Fig. 4A–C.** Micrographs from anthers of the *ms7* mutant. **A** Transmission electron microscopy of microspores showing the degenerated cytoplasm of microspores. The 'ghost' microspores remain turgid. Starch granules (arrows) accumulate in the anther wall – in the epidermis (*ep*) and endothecium (*en*). The tapetum (*t*) and middle layer (*ml*), although intact, begin to degenerate. Bar = 4 µm. **B** Microspores showing cytoplasm degeneration at the late microspore to early bicellular stage. Exine formation is complete and in some grains amyloplasts (arrows) have formed. Bars = 4 µm. **C** Scanning electron microscopy of mature anther showing pollen grains. Bar = 10 µm. **D–F** Transmission electron micrographs from wild-type anthers. Bar = 2 µm. **D** At the vacuolate microspore stage, the anther wall consists of four layers. The epidermis (*ep*) is vacuolate and contains large chloroplasts. The endothecium (*en*) also possesses large vacuoles and chloroplasts. Each cell contains prominent nucleus with a nucleolus. The middle layer (*ml*) is beginning to collapse. The tapetum cells (*t*) each contain a nucleus with a nucleolus and several small vacuoles and plastids that are beginning to differentiate into elaioplasts. **E** Microspores each possess a single large vacuole (*v*), a nucleus with nucleolus, a well-formed exine with an electron-opaque endexine (arrow) and a ribosome-rich cytoplasm with proplastids. **F** At the late microspore and early bicellular stage, the pollen grain exine is fully formed and comprises a sculptured tectum, baculae and endexine. Intine (*i*) is continuing to form and the vegetative nucleus contains a single nucleolus and is enveloped by amyloplasts (arrows) each containing many starch granules. The cytoplasm contains several small vacuoles. The tapetal cells each possess several euchromatic nuclei, elaioplasts (arrowheads) and small vacuoles. The middle-layer cytoplasm has resorbed and the cells collapsed. The epidermis and endothecium are highly vacuolate

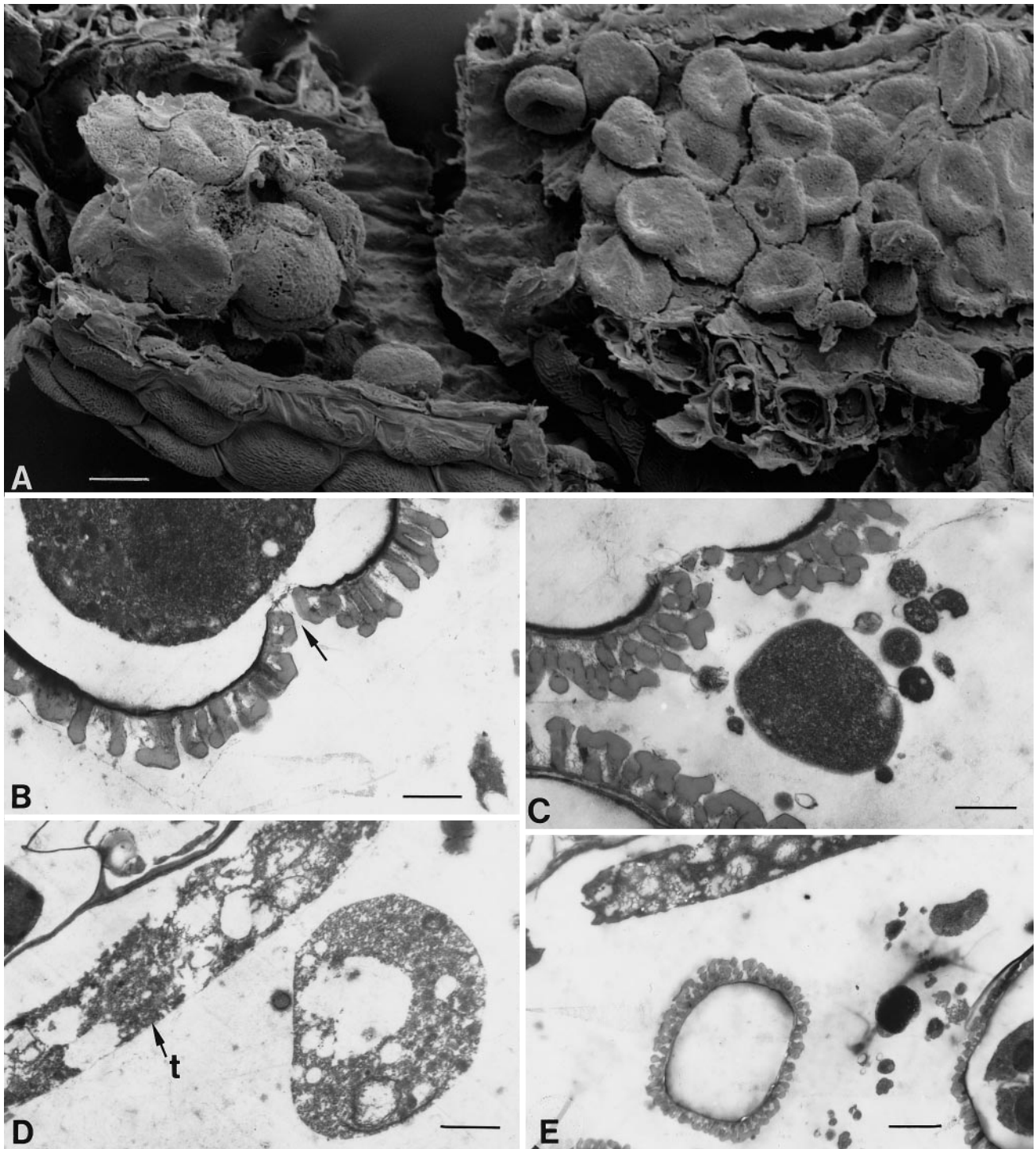


**Fig. 5A–E.** Micrographs from anthers of *ms8*. **A** Scanning electron microscopy of a mature anther showing collapsed microspores. Bar = 10  $\mu\text{m}$ . **B** Transmission electron microscopy showing the incomplete formation of the aperture (*arrow*) in the microspore. The endexine is not continuous and the cytoplasm appears to be degenerating. Bar = 1  $\mu\text{m}$ . **C** The protoplasmic contents of the microspores are often found external to the encapsulating exine, suggesting that the protoplast has exuded through the apertural zone and into the loculus. Bar = 1  $\mu\text{m}$ . **D** Many intact microspore protoplasts are found within the loculus. The tapetum (*t*) remains intact. Bar = 2  $\mu\text{m}$ . **E** The microspore ‘ghost’ exines initially appear turgid. Bar = 3  $\mu\text{m}$

Fitzgerald and Knox 1995). Although the early formation of baculae occasionally occurs in *ms9* mutants there is no further development. Like *ms12*, it is possible that there were no channels in the exine for nutrient uptake, leading to cell death. However, teratomes were not detected in *ms9*. Mutants *ms9* and *ms12* are non-allelic and, although both have impaired wall structure, they appear structurally different.

The major feature of both *ms9* and *ms12* mutants is the lack of a normal exine surrounding microspores and

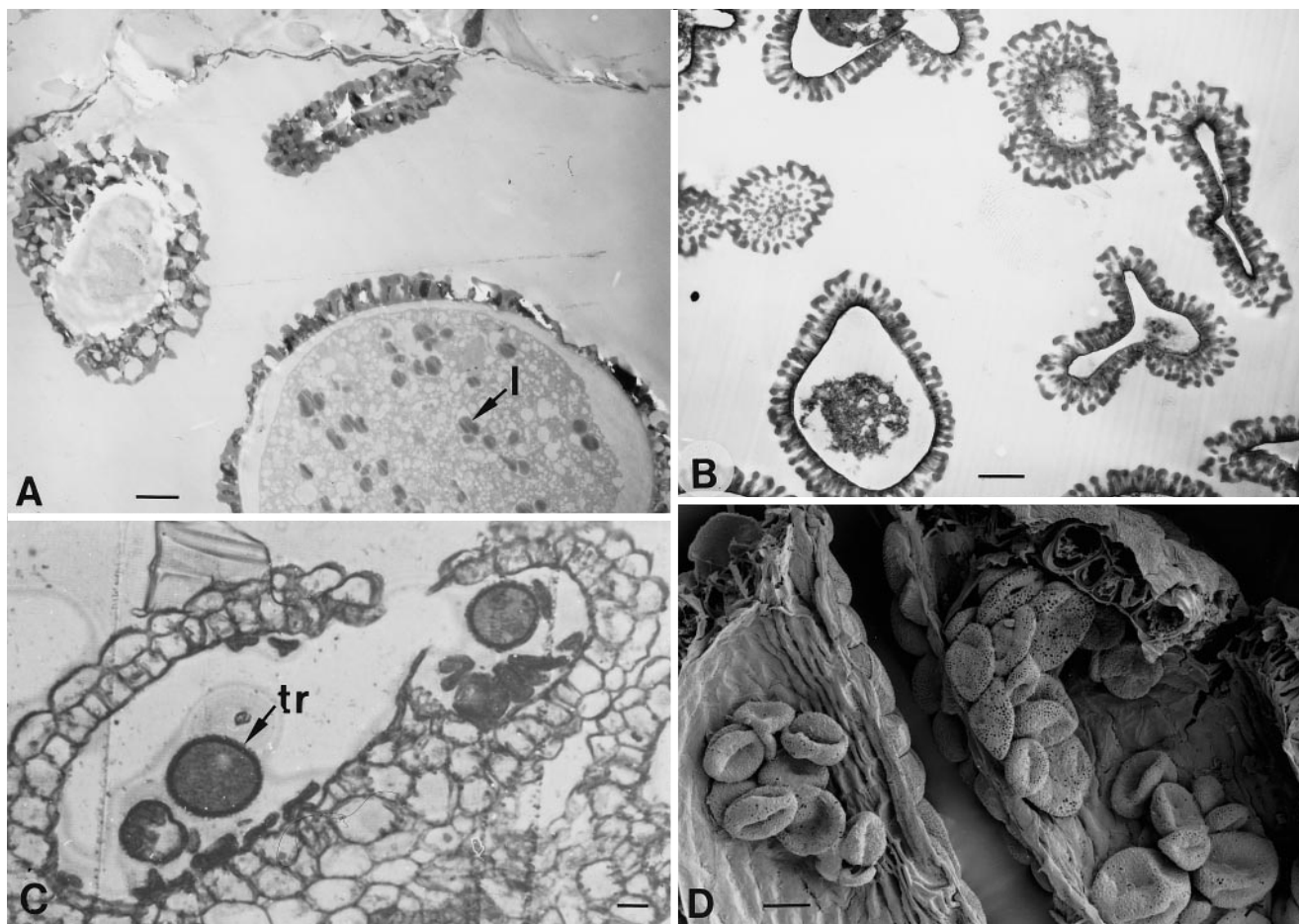
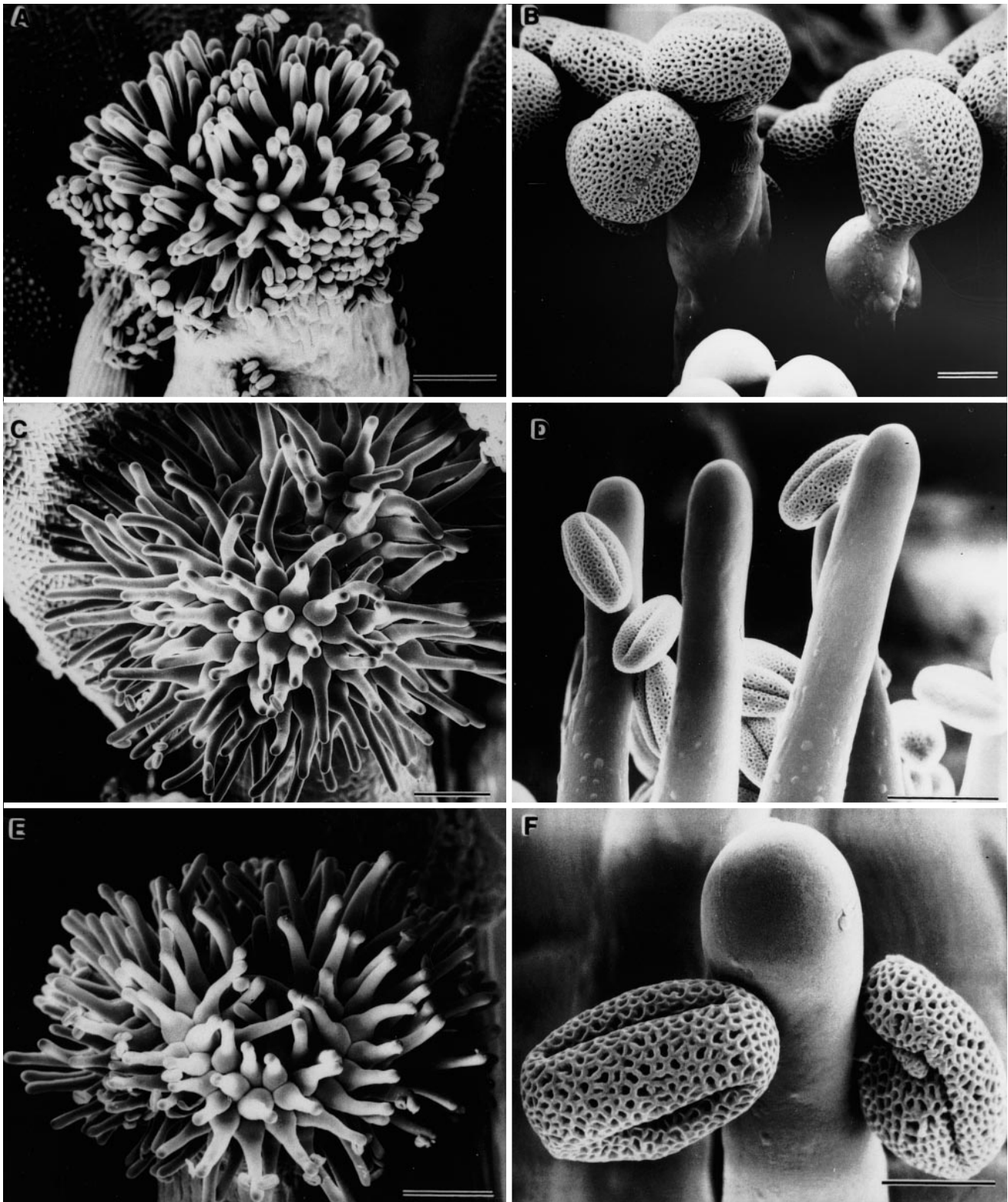


**Fig. 6A–D.** Micrographs of *ms11* anthers. **A, B** Transmission electron microscopy of microspores showing well-developed exine formation; however, most microspores collapse and their cytoplasm is resorbed. Some microspores retain intact cytoplasm comprising vesicles, lipid bodies (*l*) and mitochondria. Bars = 2  $\mu$ m. **C** Light micrograph of section of dehiscing anther, stained with Toluidine Blue, showing many collapsed microspores and a few enlarged microspores or teratomes (*tr*). **D** Mature anther (SEM) showing collapsed microspores of various sizes. Bars = 10  $\mu$ m

pollen grains. Ultrastructural studies show that the mutant microspores have a fragile exine and a vacuolate cytoplasm. However, the tapetum also appeared to degenerate at the first sign of microspore abnormality. These data suggest that exine development has been arrested at late-tetrad stage during primexine deposition with little or no tapetally derived sporopollenin having been added. In wild-type plants, primexine, made of protosporopollenin, is initially laid down prior to callose dissolution (Dahl 1986). Premature dissolution of the callose wall or the failure of a critical step in synthesis of primexine may have occurred in *ms9* and *ms12*. Both explanations are likely to involve sporophytic genes as the exine is determined sporophytically, while genes within the tapetum regulate callose breakdown. Once released from the tetrads, these microspores are unable to incorporate further tapetal sporopollenin for normal exine wall synthesis.

The callose wall is vital for production of the exine and the isolation of reproductive cells from sporophyte influence (Knox 1984; Scott et al. 1991). The callose wall consists of  $\beta$ -1,3-glucans, is secreted between the plasma membrane and the microsporocyte cell wall, and is considered to protect microspores from dehydration. The globular material surrounding the mutant microspores may be the remnants of an incomplete callose wall shown to be associated with male-sterility in other mutants (Scott et al. 1991). It is also possible that phenotypes result from early dissolution of the callose wall, prematurely releasing the tetrads of microspores and not providing them with a complete primexine and other information for normal post-tetrad survival. This observation is also consistent with the phenotype of the *msK* mutation in *Arabidopsis* (Dawson et al. 1993), which causes faulty timing of synthesis or turnover and distribution of callose.

In *ms9* and *ms12* plants, starch deposits accumulated in the anther wall during microspore development. Most starch produced by chloroplasts within the epidermis and endothecium is usually consumed by the microspores at the late microspore stage (Pacini 1990). The tapetal cells rely on surrounding tissues for their supply of photosynthetic nutrients and energy (Scott et al. 1991). An accumulation of starch in the anther wall is indicative of a blockage or diversion of metabolites, which could be occurring during prophase I of microspore meiosis.



*Early acting tapetal mutation.* The mutation in *ms8* plants appears to take effect during microspore development, prior to the bicellular pollen stage. The absence of intine coincides with the microspore wall breaking at the apertural sites and the cytoplasm being released into the locule. As in *ms7*, the remnants of 'ghost' pollen

grain are observed in the loculus at anthesis. One difference between the two mutants is that the exine collapses in *ms8*, but remains essentially rigid and intact in *ms7*. Consequently, a component necessary for exine rigidity that is present in *ms7* appears to be lacking in *ms8*.

**Fig. 7A–F.** Cryo-SEM of self-pollinated flowers from wild-type and *ms* mutant plants. **A** Deposition of pollen on a wild-type stigma. Bar = 100  $\mu$ m. **B** Detail of pollen germination on the stigmatic papillae of a wild-type plant. Bar = 25  $\mu$ m. **C** The stigma of the *ms10* mutant appears similar to that of the wild-type. Bar = 100  $\mu$ m. **D** pollen of *ms10* adheres to the papillae but fails to germinate. Bar = 25  $\mu$ m. **E** The *ms13* mutant has a stigma similar to that of the wild type. Bar = 100  $\mu$ m. **F** Detail of *ms13* pollen. Pollen adheres to the papillae surface but fails to germinate. Bar = 10  $\mu$ m

Intine synthesis is known to be controlled by gametophytic genes, yet pollen must rely upon the tapetum for the necessary supply of precursors (Knox 1984; Evans et al. 1992). Given that the *ms8* mutation is sporophytic and that the lesion is a post-meiotic one, the mutation may be affecting the tapetum. Tapetal activity is particularly critical during microspore postmeiotic development, so a tapetal gene mutation may cause deficiencies in particular biochemical and developmental events which would eventually translate to the pollen grains. This aberration may have been associated with the production of the intine during microspore maturation. The absence of pollen coat confirms the early degeneration of the tapetum.

**Late-acting tapetal mutations.** Microspores of *ms11* have developed a sculptured exine by mid-vacuolate stage. The degeneration of tapetum and microspore cytoplasm after wall formation bears some similarity to *ms7*; however, pollen grains of *ms11* collapse soon after the mutation has taken effect. A phenomenon to note in *ms11* is the occasional fully matured teratome amongst collapsed microspores. Staining of teratomes with DAPI indicates the absence of a defined nucleus. Instead, DNA is dispersed throughout the cytoplasm of the teratome, possibly contained within mitochondria and plastids. The diffuse localization of  $\beta$ -galactosidase within the locule implies that the tapetum has prematurely ruptured.

Male sterility can be a direct consequence of a tapetal aberration affecting the ability of the tapetal cells to play their crucial role in pollen development. The *ms7* mutation is apparently tapetal-specific. Early disruption of the tapetum causes death of pollen grains at around the late vacuolate to early bicellular stage

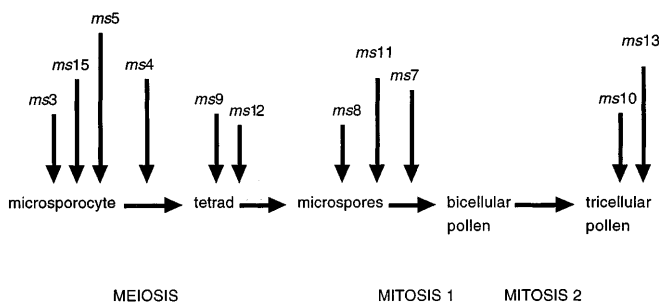


**Fig. 8.** Flow diagram of pollen developmental stages showing onset of defect for each premeiotic and postmeiotic mutant leading to male sterility (data also from Chaudhury et al. 1994)

although occasionally  $\beta$ -galactosidase and peroxidase markers at this stage show normal activity. Asynchronous development of microspores is common in anthers of both wild-type and mutant plants. Compared with fertile anthers, starch granules are formed in excess within the epidermal and endothelial cells of *ms7*, suggesting a blockage in the passage of nutrients to the microspores.

**Eceriferum mutants.** Pollen function mutants define a class of *ms* mutants that produces and releases abundant pollen that fails to germinate. Environmental conditions, such as high humidity, allow in vivo germination, and pollen from these mutants also germinates in vitro. Similar mutants have previously been isolated and found to be *eceriferum* mutants. These are mutants that have alterations in the wax layer found on stems and leaves and are typified by their bright-green stems. Twenty two different loci have been detected in *Arabidopsis* which are involved in the regulation of epicuticular wax synthesis. Only some of these *eceriferum* mutants show reduced fertility (*cer1*, *cer3*, *cer6*, *cer8* and *cer10*) (McNevin et al. 1993; Lemieux et al. 1994). Alleles of *cer1*, *cer3* and *cer6* have been identified by screening for pollen-function mutants (Preuss et al. 1993; Hülkamp et al. 1995). Sterility in all of these *eceriferum* mutants is thought to result from reduced or altered lipid and wax composition on the pollen surface (Preuss et al. 1993). The *CER1* gene has been cloned by transposon tagging. The *CER1* protein is thought to function as a decarboxylase in wax alkane synthesis (Aarts et al. 1995).

The two mutants identified in our experiments (*ms10* and *ms13*), may represent new alleles of any of these mutants or define new complementation groups. Mutant plants have the bright-green stems typifying *eceriferum* mutants. One mutant, *cer6* (*pop1*), has been previously described in detail (Preuss et al. 1993) and has a similar phenotype to *ms10*. Mutant plants of *ms10* produce viable pollen from dehisced anthers. However, abnormalities on the pollen surface of *ms10* mutants apparently restrict germination to high-humidity conditions. The results of allelism tests between *ms10* and *cer6-2* show that they are not allelic. Mapping and more allelism tests are needed to establish the number of different complementation groups defined by these pollen-function mutants.

Based on the detailed phenotypic analysis reported in this paper, the stage of defect onset for each of seven non-allelic male-sterile mutants was determined. These mutants represent complementation groups additional to the early acting mutants reported previously, *ms3*, *ms4*, *ms5* and *ms15* (Chaudhury et al. 1994). Along with *ms1* (Van der Veen and Wirtz 1968) and *antherless* (Chaudhury et al. 1992) these represent thirteen different complementation groups giving rise to nuclear male sterility in *Arabidopsis*. Presumably, this number will increase as more allelism tests are performed. Other species such as maize and tomato have approximately 60 genes that affect male fertility (Horner and Palmer 1995).



We thank the Australian Research Council for financial support and S. McCormick, the ABRC stock centre and the ABRC stock centre for providing plant material. J.A.G. was supported by an Australian Postgraduate Award administered by the Australian National University, as well as a Graduate Assistantship from the Co-operative Research Centre for Plant Science.

## References

- Aarts MGM, Corzaan P, Stiekema WJ, Pereira A (1995) A two element enhancer-inhibitor transposon system in *Arabidopsis thaliana*. *Mol Gen Genet* 247: 555–564
- Bowman JL, Drews GN, Meyerowitz EM (1991) Expression of the *Arabidopsis* floral homeotic gene *AGAMOUS* is restricted to specific cell types late in flower development. *Plant Cell* 3: 749–758
- Chaudhury A, Craig S, Blömer KC, Farrell L, Dennis ES (1992) Genetic control of male fertility in higher plants. *Aust J Plant Physiol* 19: 419–426
- Chaudhury AM, Lavithis M, Taylor PE, Craig S, Singh MB, Signer ER, Knox RB, Dennis ES (1994) Genetic control of male fertility in *Arabidopsis thaliana*: structural analysis of premeiotic developmental mutants. *Sex Plant Reprod* 7: 17–28
- Chen YC, McCormick S (1996) Sidecar pollen, an *Arabidopsis thaliana* male gametophytic mutant with aberrant cell divisions during pollen development. *Development* 122: 3243–3253.
- Craig S, Beaton, CD (1996) A simple cryo-SEM method for delicate plant tissues. *J Microsc* 182: 102–105
- Dahl AO (1986) Observation on pollen development in *Arabidopsis* under gravitationally controlled environments. In: Blackmore S, Ferguson IK (eds) *Pollen and spores: form and function*. Academic Press, London, pp 49–60
- Dawson J, Wilson ZA, Aarts MGM, Braithwaite A, Briarty LGB, Mulligan BJ (1993) Microspore and pollen development in six male-sterile mutants of *Arabidopsis thaliana*. *Can J Bot* 71: 629–638
- DeBlock M, Debrouwer D (1992) In-situ enzyme histochemistry on plastic-embedded plant material. The development of an artefact-free  $\beta$ -glucuronidase assay. *Plant J* 2: 261–266
- Evans DE, Taylor PE, Singh MB, Knox RB (1992) The interrelationship between the accumulation of lipids, protein and the level of acyl carrier protein during the development of *Brassica napus* L. pollen. *Planta* 186: 343–354
- Fitzgerald MA, Knox RB (1995) Initiation of primexine in freeze-substituted microspores of *Brassica campestris*. *Sex Plant Reprod* 8: 99–104
- Goldberg RB, Beals TP, Sanders PM (1993) Anther development: basic principles and practical applications. *Plant Cell* 5: 1217–1229
- He C, Tirlapur U, Cresti M, Peja M, Crone DE, Mascarenhas JP (1996) An *Arabidopsis* mutant showing aberrations in male meiosis. *Sex Plant Reprod* 9: 54–57
- Heslop-Harrison J (1968) Wall development within the microspore tetrad of *Lilium longiflorum*. *Can J Bot* 46: 1185–1192
- Heslop-Harrison J (1971) Wall pattern formation in angiosperm microsporogenesis. *Symp Soc Exp Biol* 25: 277–300
- Horner I, Palmer R (1995) Mechanisms of genic male-sterility. *Crop Sci* 35: 1527–1535
- Hülkamp M, Kopczak SD, Horejsi TF, Kihl BK, Pruitt RE (1995) Identification of genes required for pollen-stigma recognition in *Arabidopsis thaliana*. *Plant J* 8: 703–714
- Jefferson RA, Kavanagh TA, Bevan MW (1987) GUS fusions:  $\beta$ -glucuronidase as a sensitive and versatile gene fusion marker in higher plants. *EMBO J* 6: 3901–3907
- Knox RB (1984) The pollen grain. In: Johri JL (ed) *Embryology of angiosperms*. Springer, Berlin pp 197–271
- Lemieux B, Koornneef M, Feldmann KA (1994) Epicuticular wax & eceriferum mutants. In Meyerowitz EM, Somerville CR (eds.) *Arabidopsis* Cold Spring Harbor Press, New York, pp 1031–1047
- McNevin JP, Woodward W, Hannouf AA, Feldmann KA, Lemieux B (1993) Isolation and characterization of eceriferum (cer) mutants induced by T-DNA insertions in *Arabidopsis thaliana*. *Genome* 36: 610–618
- Muschietti J, Dircks L, Van Canneyt G, McCormick S (1994) LAT52 protein is essential for tomato pollen development. Pollen expressing antisense LAT52 RNA hydrates and germinates abnormally and cannot achieve fertilization. *Plant J* 6: 321–338
- Pacini E (1990) Tapetum and microspore function. In: Blackmore S, Knox RB (eds) *Microspores: evolution and ontogeny*. Academic Press, London, pp 213–237
- Peirson BN, Owen HA, Feldmann KA, Makaroff CA (1996) Characterization of three male-sterile mutants of *Arabidopsis thaliana* exhibiting alterations in meiosis. *Sex Plant Reprod* 9: 1–16
- Preuss D, Lemieux B, Yen G, Davis RW (1993) A conditional sterile mutation eliminates surface components from *Arabidopsis* pollen and disrupts cell signalling during fertilisation. *Genes Devel* 7: 74–985
- Regan SM, Moffat BA (1990) Cytochemical analysis of pollen development in wild-type *Arabidopsis* and a male-sterile mutant. *Plant Cell* 2: 877–889
- Scott R, Hodge R, Paul W, Draper J (1991) The molecular biology of anther differentiation. *Plant Mol Biol* 17: 195–207
- Serra, J.A. (1965) *Modern genetics*, vol 1. Academic Press, London 266–269
- Singh MB, Knox RB (1984) Quantitative cytochemistry of  $\beta$ -galactosidase in normal and enzyme deficient (gal) pollen of *Brassica campestris*: application of the indigogenic method. *Histochem J* 16: 1–24
- Stevens W.L. (1939) Tables of the recombination fraction estimated from the product ratio. *J Genet* 39: 171–180
- Twell, D (1992) Use of a nuclear-targeted  $\beta$ -glucuronidase fusion protein to demonstrate vegetative cell-specific gene expression in developing pollen. *Plant J* 2: 887–892
- Twell D, Yamaguchi J, McCormick S (1990) Pollen-specific gene expression in transgenic plants: coordinate regulation of two different tomato gene promoters during microsporogenesis. *Development* 109: 705–713
- Van der Veen JH, Wirtz P (1968) EMS-induced genetic male sterility in *Arabidopsis thaliana*: a model selection experiment. *Euphytica* 17: 371–377